Available online at www.sciencedirect.com
SCIENCE DIRECT
Journal of Sound and Vibration 294 (2006) 441–453
JOURNAL OF SOUND AND VIBRATION
www.elsevier.com/locate/jsvi

Influences of the vertical and the roll motions of frames on the hunting stability of trucks moving on curved tracks

Sen-Yung Lee*, Yung-Chang Cheng

Department of Mechanical Engineering, National Cheng Kung University, Tainan, Taiwan 701, ROC

Received 9 May 2005; received in revised form 23 September 2005; accepted 31 October 2005
Available online 19 January 2006

Abstract

Based on the heuristic nonlinear creep model, the nonlinear coupled differential equations of the motion for the truck modeled by a eight-degrees of freedom system moving on curved tracks, considering the lateral displacement and the yaw angle of the each wheelset and the lateral displacement, the vertical displacement, the roll angle and the yaw angle of the truck frame, are derived. The accuracy of the present analysis is verified by comparing the limiting case and the current numerical results with the findings available in published literature. The influences of the vertical and the roll motions of frames on the critical hunting speed of trucks are studied and evaluated via the linear and the nonlinear creep models. It is shown that the critical hunting speeds evaluated using the eight-degrees of freedom system differ significantly from those calculated using a system with six-degrees of freedom. In addition, the influences of the physical parameters, including those missing in the six-degrees of freedom system, on the critical hunting speed of trucks are also examined.

1. Introduction

In the 20th Century, the high-speed railway (HSR) has become to be one of the important transit systems. Particularly with the advent of the high-speed passenger trains, the problem of achieving high-speed operation without the hunting instability has always been of interest to vehicle designers.

The studies on the dynamic stability of a truck can be found in a number of literatures [1–16]. Recently, many researchers focused their studies on the hunting stability and dynamic analysis of trucks running on curved tracks [6–16]. In the early investigations on the hunting stability of a truck, the truck system was usually modeled by a four-degrees of freedom (4dof) or six-degrees of freedom (6dof) system. The hunting stability of a truck modeled by a 4dof system, considering the lateral displacement and the yaw angle of each wheelset, was studied by Scheffel et al. [6]. The hunting stability of a truck modeled by a 6dof system, considering the lateral displacement and the yaw angle of the each wheelset and the truck frame, was investigated by Wickens [7,8], Bell and Horak [9], Suda [10], Suda et al. [11], Fujioka et al. [12], Narayana et al. [13], Dukkipati et al. [14,15], and Lee and Cheng [16].

*Corresponding author. Fax: 886 6 2352973.
E-mail address: sylee@mail.ncku.edu.tw (S.-Y. Lee).

0022-460X/$ - see front matter © 2005 Elsevier Ltd. All rights reserved.
doi:10.1016/j.jsv.2005.10.025

Nomenclature

a half of the track gauge
b_1 half of the primary yaw spring arm and the primary yaw damping arm
b_1 half of the primary vertical spring arm and the primary vertical damping arm
b_2 half of the secondary longitudinal spring arm
b_3 half of the secondary longitudinal damping arm
C_{px} yaw damping of the primary suspension
C_{py} lateral damping of the primary suspension
C_{pz} vertical damping of the secondary suspension
C_{sx} yaw damping of the secondary suspension
C_{sy} lateral damping of the secondary suspension
f_{11} lateral creep force coefficient
f_{12} lateral/spin creep force coefficient
f_{22} spin creep force coefficient
f_{33} longitudinal creep force coefficient
F_{gi} lateral gravitational stiffness of the front wheelset and the rear wheelset, respectively, $i = 1, 2$
F_{jxi} linear creep force of front and rear wheelset ($i = 1, 2$, respectively) in longitudinal direction of left and right wheel ($j = \mathrm{L}, \mathrm{R}$, respectively)
F_{jyi} linear creep force of front and rear wheelset ($i = 1, 2$, respectively) in lateral direction of left and right wheel ($j = \mathrm{L}, \mathrm{R}$, respectively)
F^n_{jxi} nonlinear creep force of front and rear wheelset ($i = 1, 2$, respectively) in longitudinal direction of left and right wheel ($j = \mathrm{L}, \mathrm{R}$, respectively)
F^n_{jyi} nonlinear creep force of front and rear wheelset ($i = 1, 2$, respectively) in lateral direction of left and right wheel ($j = \mathrm{L}, \mathrm{R}$, respectively)
F^*_{jxi} linear creep force of front and rear wheelset ($i = 1, 2$, respectively) as given directly by Kalker's linear theory in longitudinal direction of left and right wheel ($j = \mathrm{L}, \mathrm{R}$, respectively)
F^*_{jyi} linear creep force of front and rear wheelset ($i = 1, 2$, respectively) as given directly by Kalker's linear theory in lateral direction of left and right wheel ($j = \mathrm{L}, \mathrm{R}$, respectively)
F_{syi} suspension force of front and rear wheelset ($i = 1, 2$, respectively) in lateral direction
F_{syt} suspension force of truck frame in lateral direction
F_{szt} suspension force of truck frame in vertical direction
F_{ti} flange contact force
h_T vertical distance from the wheelset center of the gravity to the secondary suspension
I_{tx} roll moment of inertia of the truck frame
I_{tz} yaw moment of the inertia of the truck frame
I_{wx} roll moment of the inertia of the wheelset
I_{wy} spin moment of the inertia of the wheelset
I_{wz} yaw moment of the inertia of the wheelset
K_r lateral rail stiffness
K_{px} longitudinal stiffness of the primary suspension
K_{py} lateral stiffness of the primary suspension
K_{pz} vertical stiffness of the secondary suspension
K_{sx} longitudinal stiffness of the secondary suspension
K_{sy} lateral stiffness of the secondary suspension
L_1 half of the primary lateral spring arm
L_2 half of the primary lateral damping arm
m_c car body mass
m_t bogie frame mass
m_w wheelset mass
M_{gi} yaw gravitational stiffness of the front wheelset and the rear wheelset, respectively, $i = 1, 2$
M_{jzi} linear creep moment of front and rear wheelset ($i = 1, 2$, respectively) in vertical direction on left and right wheel ($j = \mathrm{L}, \mathrm{R}$, respectively)
M^n_{jzi} nonlinear creep moment of front and rear wheelset ($i = 1, 2$, respectively) in vertical direction of left and right wheel ($j = \mathrm{L}, \mathrm{R}$, respectively)
M^*_{jzi} linear creep moment of front and rear wheelset ($i = 1, 2$, respectively) as given

directly by Kalker's linear theory in vertical direction of left and right wheel ($j = \mathrm{L}, \mathrm{R}$, respectively)

M_{szi} suspension moment of front and rear wheelset ($i = 1, 2$, respectively) in vertical direction

M_{sxt} suspension moment of truck frame in longitudinal direction

M_{szt} suspension moment of truck frame in vertical direction

N normal force of the wheelset at the equilibrium state

N_{Li} normal force on left wheel of front and rear wheelset ($i = 1, 2$, respectively) in lateral direction

N_{Ri} normal force on right wheel of front and rear wheelset ($i = 1, 2$, respectively) in lateral direction

r_L left wheel rolling radius

r_R right wheel rolling radius

r_0 nominal wheelset rolling radius

R radius of the curved track

R_{Lxi} x component of position vector on left wheel of front and rear wheelset ($i = 1, 2$, respectively)

R_{Lyi} y component of position vector on left wheel of front and rear wheelset ($i = 1, 2$, respectively)

R_{Rxi} x component of position vector on right wheel of front and rear wheelset ($i = 1, 2$, respectively)

R_{Ryi} y component of position vector on right wheel of front and rear wheelset ($i = 1, 2$, respectively)

t time

V forward speed of the truck

V_{cr} critical speed

W axle load

x longitudinal coordinate

y lateral coordinate

y_i lateral displacement of front and rear wheelset ($i = 1, 2$, respectively)

y_t lateral displacement of the truck

z vertical coordinate

z_t vertical displacement of the truck frame

α_i saturation constant of nonlinear creep force model of the front wheelset and the rear wheelset, respectively, $i = 1, 2$

β_i nonlinearity of nonlinear creep force model of the front wheelset and the rear wheelset, respectively, $i = 1, 2$

β_{ji} nonlinearity of nonlinear creep force model of the left wheel and the right wheel of the front wheelset and the rear wheelset, respectively, $i = 1, 2$, and $j = \mathrm{L}, \mathrm{R}$

δ flange clearance between the wheel and the rail

δ_L contact angle of the left wheel

δ_R contact angle of the right wheel

λ wheel conicity

ϕ_{se} superelevation angle of curved tracks

ϕ_t roll angle of the truck frame

ψ_i yaw angle of front and rear wheelset, respectively ($i = 1, 2$, respectively)

ψ_t yaw angle of the truck frame

Based on the linear creep model without considering the creep moments between wheels and rails, the curving performance of the unsymmetric truck was presented by Wickens [7,8]. The dynamic stability of a truck with variable yaw constraint suspension was studied by Scheffel et al. [6]. It is shown that the variable yaw constrain suspension system can increase the steady-state curving performance. In order to improve the dynamic stability of vehicles, a forced steering bogie was used. The dynamic stability of a forced steering truck without considering spin creepages was investigated by Bell and Horak [9]. Suda [10] and Fujioka et al. [12] examined the dynamic stability of unconventional trucks, including the linkage or the unsymmetric suspensions.

It is well known that the new HSR systems are connected with nonlinear physical parameters. However, the nonlinear analysis on the dynamic stability of the truck system is insufficient. Based on the nonlinear creep model, the steady-state curving performance of a non-linkage truck and a linkage truck was compared by Suda et al. [11]. Utilizing the heuristic nonlinear creep model, Narayana et al. [13] and Dukkipati et al. [14,15] illustrated the steady-state curving behavior of a conventional truck and an unconventional truck. The comparative study on the steady-state curving performance and the dynamic stability of some unconventional trucks designs was investigated. Recently, Lee and Cheng [16] investigated the influence of the suspension parameters on the critical hunting speed of a truck considering the nonlinear creep moments.

An important aspect for the hunting stability analysis of HSR vehicle systems is the consideration of the vertical and the roll motions of frames of the trucks. However, a review of the existing literature reveals that previous studies into the hunting stability of a truck moving on curved tracks have never adopted the 8dof systems required to take these two parameters into consideration. Moreover, even though the equations of the motion of a 6dof system can be found in the book given by Dukkipati and Garg [17], the equations of motion of a truck frame considering the vertical displacement and the roll angle were not derived. Additionally, the suspension forces in the vertical direction and the suspension moments in the longitudinal direction of the truck were also neglected.

In this paper, one assumes that the wheels of the truck will not lose contact with the rail. This paper adopts the heuristic nonlinear creep model to derive the governing differential equations of motion for a truck modeled by a 8dof system moving on curved tracks. To verify the accuracy of the present analysis, the limiting case is examined. The numerical result is compared with the finding available in existing literature. The Lyapunov indirect method is utilized to evaluate and compare the influences of several physical parameters on the critical hunting speeds for the 6dof and 8dof systems. Finally, the influences of the physical parameters, including those missing in the 6dof system, on the critical hunting speed are also examined.

2. Differential equations of motion

Figs. 1 and 2 illustrate the truck system considered in the present study. The governing equations of motion for the lateral displacement y_t, the vertical displacement z_t, the roll angle ϕ_t and the yaw angle ψ_t of the truck

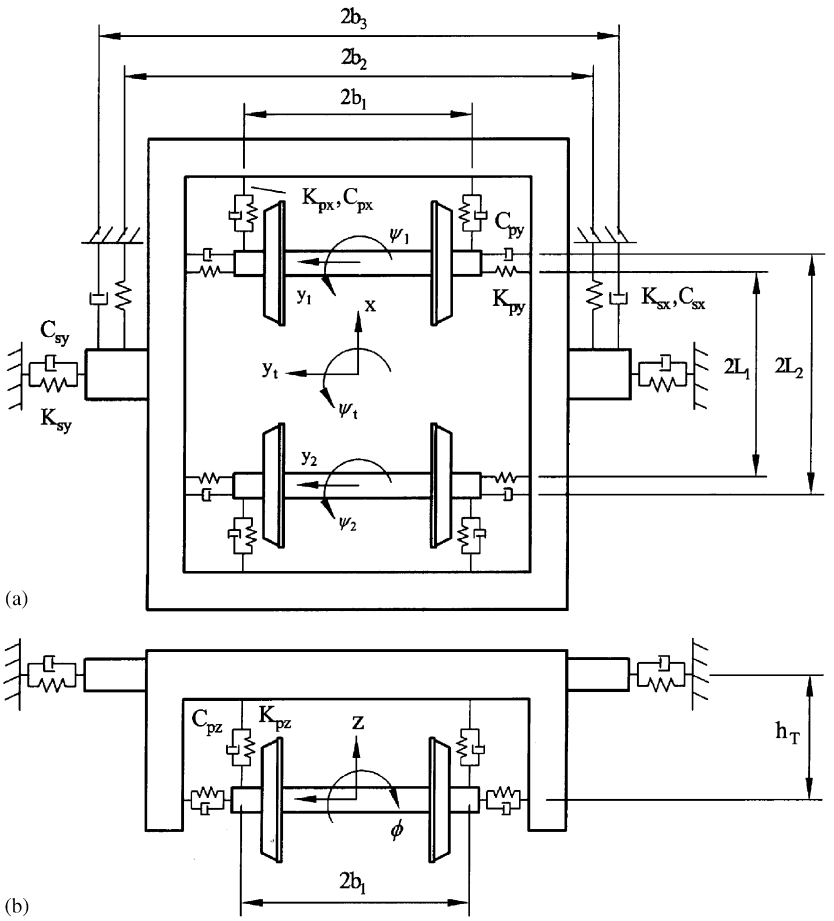

Fig. 1. Two-axle truck model.

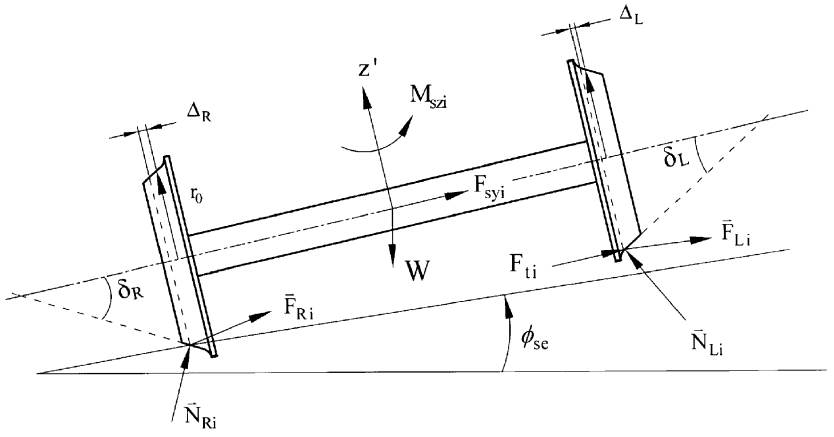

Fig. 2. The free body diagram of a single wheelset.

frame are given by

$$m_t\ddot{y}_t = F_{syt} + \left(m_t + \frac{m_c}{2}\right)\left(\frac{V^2}{gR} - \phi_{se}\right)g, \tag{1}$$

$$m_t\ddot{z}_t = F_{szt} + \left(m_t + \frac{m_c}{2}\right)\left(\frac{V^2}{gR}\,\phi_{se} + 1\right)g, \tag{2}$$

$$I_{tx}\ddot{\phi}_t = M_{sxt}, \tag{3}$$

$$I_{tz}\ddot{\psi}_t = M_{szt}, \tag{4}$$

where V is the speed of motion, R is the radius of curved tracks and ϕ_{se} is the superelevation angle of curved tracks. The physical quantities $F_{syt}, F_{szt}, I_{tx}, I_{tz}, M_{sxt}, M_{szt}$, and m_t are defined in the nomenclature. It is noted that in Eqs. (1)–(4), the dots indicate differentiation with respect to the time variable t.

Adopting the notations used by Dukkipati and Garg [17], when the inertia forces and the heuristic nonlinear creep forces and moments are considered, the governing coupled differential equations of motion for the lateral displacement y_i and the yaw angle ψ_i, of the wheelsets are coupled differential equations

$$m_w\left(\ddot{y}_i - \frac{V^2}{R} + g\phi_{se}\right) = F^n_{Lyi}(y_i,\dot{y}_i,\psi_i,\dot{\psi}_i) + F^n_{Ryi}(y_i,\dot{y}_i,\psi_i,\dot{\psi}_i) - F_{gi} + F_{syi} - F_{ti}, \tag{5}$$

$$\begin{aligned} I_{wz}\ddot{\psi}_i = & -I_{wy}\frac{V}{r_0}\dot{\phi}_i + [R_{Rxi}F^n_{Ryi}(y_i,\dot{y}_i,\psi_i,\dot{\psi}_i) - R_{Ryi}F^n_{Rxi}(y_i,\dot{y}_i,\psi_i,\dot{\psi}_i)] \\ & + [R_{Lxi}F^n_{Lyi}(y_i,\dot{y}_i,\psi_i,\dot{\psi}_i) - R_{Lyi}F^n_{Lxi}(y_i,\dot{y}_i,\psi_i,\dot{\psi}_i)] \\ & - M_{gi} + M^n_{Lzi}(y_i,\dot{y}_i,\psi_i,\dot{\psi}_i) + M^n_{Rzi}(y_i,\dot{y}_i,\psi_i,\dot{\psi}_i) + M_{szi}, \end{aligned} \tag{6}$$

where the subscript i, $i = 1, 2$, in the physical quantities in this paper represent the corresponding physical quantities of the front and the rear wheelset, respectively. ϕ_i is the roll angle of the wheelset and $\phi_i = (\lambda/a)y_i$. λ is the conicity angle and a is the half of track gauge. $F^n_{Rxi}(y_i,\dot{y}_i,\psi_i,\dot{\psi}_i)$, $F^n_{Ryi}(y_i,\dot{y}_i,\psi_i,\dot{\psi}_i)$, $F^n_{Lxi}(y_i,\dot{y}_i,\psi_i,\dot{\psi}_i)$ and $F^n_{Lyi}(y_i,\dot{y}_i,\psi_i,\dot{\psi}_i)$ are the x and the y components of the creep forces of the right wheel and the left wheel, respectively, $M^n_{Rzi}(y_i,\dot{y}_i,\psi_i,\dot{\psi}_i)$ and $M^n_{Lzi}(y_i,\dot{y}_i,\psi_i,\dot{\psi}_i)$ are the creep moments in the z direction with respect to the right wheel and the left wheel, respectively. The other physical parameters, such as, $F_{gi}, F_{syi}, F_{ti}, I_{wy}, I_{wz}, M_{gi}, M_{sxi}, m_w, r_0, R_{Lxi}, R_{Lyi}, R_{Rxi}$ and R_{Ryi} are all defined in the nomenclature.

A heuristic nonlinear creep model, which combines the Kalker's linear creep theory with a creep force saturation representation, is used in the analysis. The nonlinear creep forces and the nonlinear creep moments

are given as [2]

$$F^n_{jxi}(y_i,\dot{y}_i,\psi_i,\dot{\psi}_i)=\alpha_i F_{jxi}, \tag{7a}$$

$$F^n_{jyi}(y_i,\dot{y}_i,\psi_i,\dot{\psi}_i)=\alpha_i F_{jyi}, \tag{7b}$$

$$M^n_{jzi}(y_i,\dot{y}_i,\psi_i,\dot{\psi}_i)=\alpha_i M_{jzi}, \tag{7c}$$

where the subscript j, $j=\mathrm{L},\mathrm{R}$, in the physical quantities in this paper represent the corresponding physical quantities of the right wheel and the left wheel, respectively. F_{jxi}, F_{jyi} and M_{jzi} are the linear creep forces and the linear creep moments and are given as

$$\begin{aligned}F_{Lxi}=&-\frac{f_{33}}{V}\left[V\left(1+\frac{a}{R}-\frac{r_L}{r_0}\right)-a\dot{\psi}_i\right]\\&+\frac{f_{11}}{V}\psi_i(\dot{y}_i-V\psi_i+r_L\dot{\phi}_i)+\frac{f_{12}}{V}\psi_i\left[\left(\dot{\psi}_i-\frac{V}{R}\right)-\frac{V}{r_0}\delta_L\right],\end{aligned} \tag{8a}$$

$$\begin{aligned}F_{Lyi}=&-\frac{f_{33}}{V}\psi_i\left[V\left(1+\frac{a}{R}-\frac{r_L}{r_0}\right)-a\dot{\psi}_i\right]\\&-\frac{f_{11}}{V}(\dot{y}_i-V\psi_i+r_L\dot{\phi}_i)-\frac{f_{12}}{V}\left[\left(\dot{\psi}_i-\frac{V}{R}\right)-\frac{V}{r_0}\delta_L\right],\end{aligned} \tag{8b}$$

$$M_{Lzi}=\frac{f_{12}}{V}(\dot{y}_i-V\psi_i+r_L\phi_i)-\frac{f_{22}}{V}\left[\left(\dot{\psi}_i-\frac{V}{R}\right)-\frac{V}{r_0}\delta_L\right], \tag{8c}$$

$$\begin{aligned}F_{Rxi}=&-\frac{f_{33}}{V}\left[V\left(1-\frac{a}{R}-\frac{r_R}{r_0}\right)+a\dot{\psi}_i\right]\\&+\frac{f_{11}}{V}\psi_i(\dot{y}_i-V\psi_i+r_R\dot{\phi}_i)+\frac{f_{12}}{V}\psi_i\left[\left(\dot{\psi}_i-\frac{V}{R}\right)+\frac{V}{r_0}\delta_R\right],\end{aligned} \tag{9a}$$

$$\begin{aligned}F_{Ryi}=&-\frac{f_{33}}{V}\psi_i\left[V\left(1-\frac{a}{R}-\frac{r_R}{r_0}\right)+a\dot{\psi}_i\right]\\&-\frac{f_{11}}{V}(\dot{y}_i-V\psi_i+r_R\dot{\phi}_i)-\frac{f_{12}}{V}\left[\left(\dot{\psi}_i-\frac{V}{R}\right)+\frac{V}{r_0}\delta_R\right],\end{aligned} \tag{9b}$$

$$M_{Rzi}=\frac{f_{12}}{V}(\dot{y}_i-V\psi_i+r_R\phi_i)-\frac{f_{22}}{V}\left[\left(\dot{\psi}_i-\frac{V}{R}\right)+\frac{V}{r_0}\delta_R\right]. \tag{9c}$$

The saturation constant α_i is [2]

$$\alpha_i=\begin{cases}\dfrac{1}{\beta_i}\left[\beta_i-\dfrac{1}{3}\beta_i^2+\dfrac{1}{27}\beta_i^3\right] & \text{for } \beta_i\leqslant 3,\\ \dfrac{1}{\beta_i} & \text{for } \beta_i\geqslant 3,\end{cases} \tag{10}$$

where

$$\beta_i=\frac{\beta_{Ri}+\beta_{Li}}{2} \tag{11}$$

and

$$\beta_{ji}=\frac{\sqrt{(F^*_{jxi})^2+(F^*_{jyi})^2}}{\mu N}, \tag{12}$$

where F^*_{jxi} and F^*_{jyi} are the linear creep forces given by the Kalker's linear theory [17]

$$F^*_{Lxi} = -\frac{f_{33}}{V}\left[V\left(1+\frac{a}{R}-\frac{r_L}{r_0}\right)-a\dot{\psi}_i\right], \tag{13a}$$

$$F^*_{Lyi} = -\frac{f_{11}}{V}(\dot{y}_i + r_L\dot{\phi}_i - V\psi_i) - \frac{f_{12}}{V}\left(\dot{\psi}_i - \frac{V}{R} - \frac{V}{r_0}\,\delta_L\right), \tag{13b}$$

$$F^*_{Rxi} = -\frac{f_{33}}{V}\left[V\left(1-\frac{a}{R}-\frac{r_R}{r_0}\right)+a\dot{\psi}_i\right], \tag{14a}$$

$$F^*_{Ryi} = -\frac{f_{11}}{V}(\dot{y}_i + r_R\dot{\phi}_i - V\psi_i) - \frac{f_{12}}{V}\left(\dot{\psi}_i - \frac{V}{R} + \frac{V}{r_0}\,\delta_R\right). \tag{14b}$$

The linear lateral gravitational stiffness, F_{gi}, and the yaw gravitational stiffness, M_{gi}, are given as [17].

$$\begin{aligned} F_{gi} &= -N_{Ri}\sin(\delta_R-\phi_i) + N_{Li}\sin(\delta_L+\phi_i) \\ &\approx \left[m_w\left(\frac{V^2}{R}\right)\phi_{se} + W\right]\left[\frac{1}{2}(\delta_R-\delta_L)-\phi_i\right] \end{aligned} \tag{15}$$

and

$$\begin{aligned} M_{gi} &= R_{Lxi}N_{Li}\sin(\delta_L+\phi_i) - R_{Rxi}N_{Ri}\sin(\delta_R-\phi_i) \\ &\approx a\psi_i\left[m_w\left(\frac{V^2}{R}\right)\phi_{se} + W\right]\left[\frac{1}{2}(\delta_R+\delta_L)\right], \end{aligned} \tag{16}$$

respectively.

From Fig. 1, the suspension forces of the wheelsets in the lateral direction, F_{syi}, the suspension moments of the wheelsets in the vertical direction, M_{szi}, and the suspension forces of the truck frame in the lateral direction, F_{syt}, the suspension moments of the truck frame in the vertical direction, M_{szt}, are

$$\begin{aligned} F_{syi} = &-2K_{py}y_i - (-1)^i 2K_{py}L_1\psi_t + 2K_{py}y_t - 2C_{py}\dot{y}_i - (-1)^i 2C_{py}L_2\dot{\psi}_t + 2C_{py}\dot{y}_t \\ &+ 2C_{py}\dot{\phi}_t h_T + 2K_{py}\phi_t h_T, \end{aligned} \tag{17}$$

$$M_{szi} = 2K_{px}b^2\psi_t - 2K_{px}b^2\psi_i + 2C_{px}b_1^2\dot{\psi}_t - 2C_{px}b_1^2\dot{\psi}_i, \tag{18}$$

$$\begin{aligned} F_{syt} = &\,2K_{py}y_1 + 2C_{py}\dot{y}_1 + 2K_{py}y_2 + 2C_{py}\dot{y}_2 + (-4K_{py}-2K_{sy})y_t + (-4C_{py}-2C_{sy})\dot{y}_t \\ &- 4C_{py}\dot{\phi}_t h_T - 4K_{py}\phi_t h_T, \end{aligned} \tag{19}$$

$$\begin{aligned} M_{szt} = &(-4K_{py}L_1^2 - 4K_{px}b_1^2 - 2K_{sx}b_2^2)\psi_t + (-4C_{py}L_2^2 - 4C_{px}b_1^2 - 2C_{sx}b_3^2)\dot{\psi}_t \\ &+ 2K_{py}L_1y_1 + 2C_{py}L_2\dot{y}_1 + 2K_{px}b_1^2\psi_1 + 2C_{px}b_1^2\dot{\psi}_1 \\ &- 2K_{py}L_1y_2 - 2C_{py}L_2\dot{y}_2 + 2K_{px}b_1^2\psi_2 + 2C_{px}b_1^2\dot{\psi}_2. \end{aligned} \tag{20}$$

It should be mentioned that the physical quantities indicated as Eqs. (7)–(20), except Eqs. (17) and (19), are established previously by Dukkipati and Garg [17] and Lee and Cheng [16], who neglected the vertical stiffness and the vertical damping of the primary suspension in their system. From Fig. 1, the suspension forces of the truck frame in the vertical direction, F_{szt}, and the suspension moments of the truck frame in the longitudinal direction, M_{sxt}, acting on the truck frame, induced from the vertical stiffness and the vertical damping of the secondary suspension, and can be expressed as

$$F_{szt} = -4C_{pz}\dot{z}_t - 4K_{pz}z_t \tag{21}$$

and

$$M_{sxt} = -4C_{pz}\dot{\phi}_t b_1^2 - 4K_{pz}\phi_t b_1^2 + 2K_{py}[-2y_t + (y_1 + y_2) - 2\phi_t h_T]h_T + 2C_{py}[-2\dot{y}_t + (\dot{y}_1 + \dot{y}_2) - 2\dot{\phi}_t h_T]h_T, \tag{22}$$

respectively. The flange contact force, F_{ti}, is given by Mehdi and Shaopu [4] as

$$F_{ti} = \begin{cases} K_r(y_i - \delta), & y_i > \delta, \\ 0, & -\delta \leqslant y_i \leqslant \delta, \\ -K_r(y_i + \delta), & y_i < -\delta, \end{cases} \tag{23}$$

where δ is the flange clearance between the wheel and the rail.

For simplicity, it is assumed that the constraint function is linear for a conical wheel on a knife-edged rail. Hence, the following assumptions regarding the wheel and rail geometry can be employed:

$$\delta_L = \delta_R = \lambda, \quad \tfrac{1}{2}(r_L - r_R) = \lambda y_i, \quad \tfrac{1}{2}(r_L + r_R) = r_0. \tag{24}$$

After substituting the equations given above into Eqs. (5)–(6) and neglecting the high-order terms, one obtains the following coupled linear differential equations:

$$m_w\ddot{y}_i = -\frac{2\alpha_i f_{11}}{V}\dot{y}_i + 2\alpha_i f_{11}\psi_i - \frac{2\alpha_i f_{12}}{V}\dot{\psi}_i - \left(m_w\frac{V^2}{R}\phi_{se} + W\right)\left(\frac{\lambda}{a}y_i\right) - \frac{2r_0\alpha_i f_{11}}{V}\left(\frac{\lambda}{a}\right)\dot{y}_i + \frac{m_w V^2}{R} + \frac{2\alpha_i f_{12}}{R} - m_w g\phi_{se} + F_{syi} - F_{ti}, \tag{25}$$

$$I_{wz}\ddot{\psi}_i = \frac{2a\alpha_i f_{33}\lambda}{r_0}y_i + \frac{2\alpha_i f_{12}}{V}\dot{y}_i + \left[-2\alpha_i f_{12} + a\lambda\left(m_w\frac{V^2}{R}\phi_{se} + W\right)\right]\psi_i + \left(-\frac{2a^2\alpha_i f_{33}}{V} - \frac{2\alpha_i f_{22}}{V}\right)\dot{\psi}_i + \left[-\frac{I_{wy}V}{r_0} + \frac{2r_0\alpha_i f_{12}}{V}\right]\left(\frac{\lambda}{a}\right)\dot{y}_i + \frac{2\alpha_i}{R}(a^2 f_{33} + f_{22}) + M_{szi}, \tag{26}$$

where $\alpha_i = \alpha_i(y_i, \dot{y}_i, \psi_i, \dot{\psi}_i)$. As a result, Eqs. (1)–(4) and (25)–(26) form the eight governing differential equations of motion of the system. When $\alpha_i = 1$, $\phi_{se} = 0$, R is set to be infinite, and the vertical displacement and the roll angle of the truck are neglected, the nonlinear differential equations can be reduced to the governing differential equations of the motion of wheelsets moving on tangent tracks, based on the linear creep model,

$$m_w\ddot{y}_i = -\frac{2f_{11}}{V}\dot{y}_i + 2f_{11}\psi_i - \frac{2f_{12}}{V}\dot{\psi}_i - W\frac{\lambda}{a}y_i - \frac{2r_0 f_{11}}{V}\left(\frac{\lambda}{a}\right)\dot{y}_i - F_{ti} - 2K_{py}y_i - (-1)^i 2K_{py}L_1\psi_t + 2K_{py}y_t - 2C_{py}\dot{y}_i - (-1)^i 2C_{py}L_2\dot{\psi}_t + 2C_{py}\dot{y}_t, \tag{27}$$

$$I_{wz}\ddot{\psi}_i = -\frac{2af_{33}\lambda}{r_0}y_i + \frac{2f_{12}}{V}\dot{y}_i + (-2f_{12} + a\lambda W)\psi_i + \left(-\frac{2a^2 f_{33}}{V} - \frac{2f_{22}}{V}\right)\dot{\psi}_i + \left[\frac{I_{wy}V}{r_0} + \frac{2r_0 f_{12}}{V}\right]\left(\frac{\lambda}{a}\right)\dot{y}_i + M_{szi} \tag{28}$$

and the differential equation of the motion of the truck moving on tangent tracks in lateral direction is simplified as

$$m_t\ddot{y}_t = 2K_{py}y_1 + 2C_{py}\dot{y}_1 + 2K_{py}y_2 + 2C_{py}\dot{y}_2 + (-4K_{py} - 2K_{sy})y_t + (-4C_{py} - 2C_{sy})\dot{y}_t. \tag{29}$$

Eqs. (29), (4), (27) and (28), are the governing differential equations of the motion of a truck modeled by a 6dof system. These equations are identical to those given by Mehdi and Shaopu [4].

3. Stability analysis

In this paper, the Lyapunov indirect method [18] is used to study the influence of the physical parameters on the critical hunting speed of trucks. The equations of motion of the autonomous system, Eqs. (1)–(4) and (25)–(26), can be re-expressed as a system of first-order differential equations

$$\dot{\mathbf{x}}(t) = \mathbf{f}[\mathbf{x}(t)], \tag{30}$$

where $\mathbf{x}(t)$ is a 16×1 vector of state variables.

For any given velocity V, one defines a determinant matrix $\mathbf{A}$

$$\mathbf{A} = \left[\frac{\partial \mathbf{f}(\mathbf{x})}{\partial \mathbf{x}}\right]_{\mathbf{x}=\mathbf{x}_0}, \tag{31}$$

where $\mathbf{x}_0 = [X_{1,0}, X_{2,0}, X_{3,0}, \ldots, X_{16,0}]$ is the equilibrium point and satisfies $\mathbf{f}[\mathbf{x}_0] = \mathbf{0}$. The dynamic system will be unstable if any one of the eigenvalues of matrix $\mathbf{A}$ has positive real part. The lowest velocity for which the eigenvalues of associated determinant matrix $\mathbf{A}$ has non-positive real part is the critical hunting speed.

4. Numerical results

To illustrate the reliability of the numerical analysis, one compares the critical hunting speed of the reduced 6dof truck moving on a straight track, with that studied by Mehdi and Shaopu [4]. The critical speed obtained in the present analysis is 118 km/h. This result is the same as that obtained by Mehdi and Shaopu [4].

When the vertical and the roll motions of frames are also considered in the truck of 6dof system, the number of dof of the dynamic system turns to be eight. The vertical stiffness and the vertical damping of the primary suspension are the physical parameters not considered in the 6dof system. A review of the available literature reveals that the influences of these two physical parameters on the critical hunting speeds of the truck moving on curved tracks have not been investigated before.

In the following, one uses the data of the system parameters listed in appendix [19,20], except the specified ones, to study the influences of physical parameters on the critical hunting speed of a freight truck.

Fig. 3 shows the influences of the longitudinal stiffness of the primary suspension K_{px} on the critical hunting speeds of the 6dof and the 8dof truck systems evaluated via the linear and the nonlinear creep models,

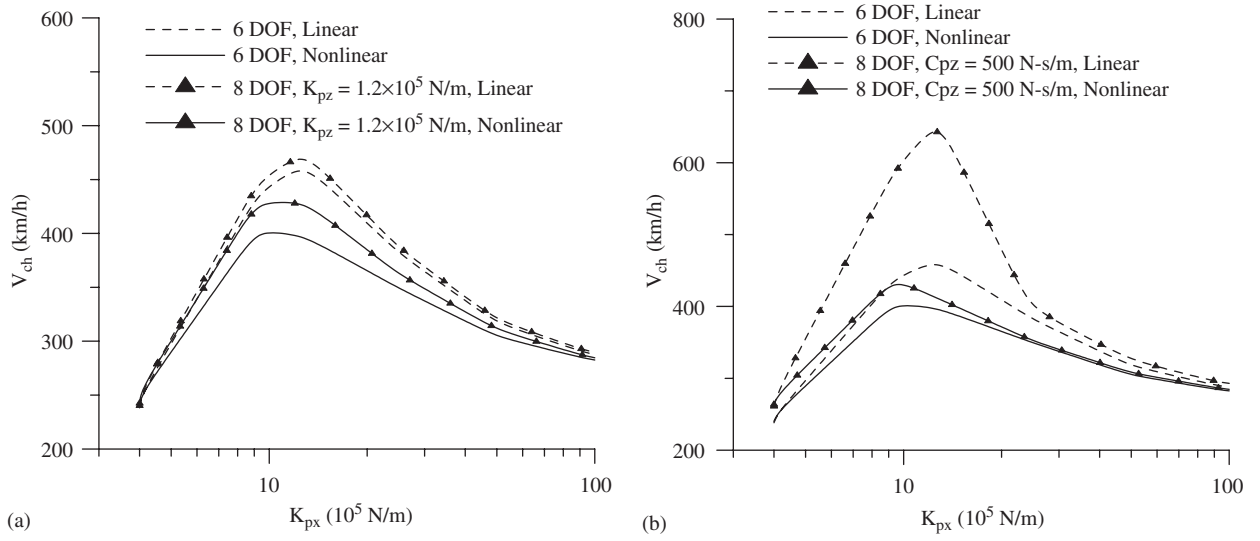

Fig. 3. The influence of the longitudinal stiffness of the primary suspension K_{px} on the critical speeds of a truck evaluated via the various degrees of freedom with the linear and the nonlinear creep models when (a) $C_{pz} = 1.44 \times 10^4$ N s/m, and (b) $K_{pz} = 2.0 \times 10^5$ N/m.

respectively. It is observed that for both 6dof and 8dof systems, the critical hunting speeds evaluated by the linear creep model are always higher than those evaluated by the nonlinear creep model. Meanwhile, in both linear and nonlinear analysis, the critical hunting speeds evaluated by the 8dof system always exceed those evaluated by the 6dof system. It can also be found that the critical hunting speeds and the difference between the two sets of critical hunting speeds will increase first then decrease as K_{px} increases.

In Fig. 4, the influences of the longitudinal damping of the secondary suspension, C_{sx}, on the critical hunting speeds are shown. It is observed that the critical hunting speeds rise monotonically as C_{sx} increases. In both linear and nonlinear analysis, the critical hunting speeds evaluated by the 8dof system always exceed those evaluated by the 6dof system. Based on the system data given in Fig. 4b, it is observed that for both 6dof and 8dof systems, the critical hunting speeds evaluated by the linear creep model are always higher than those

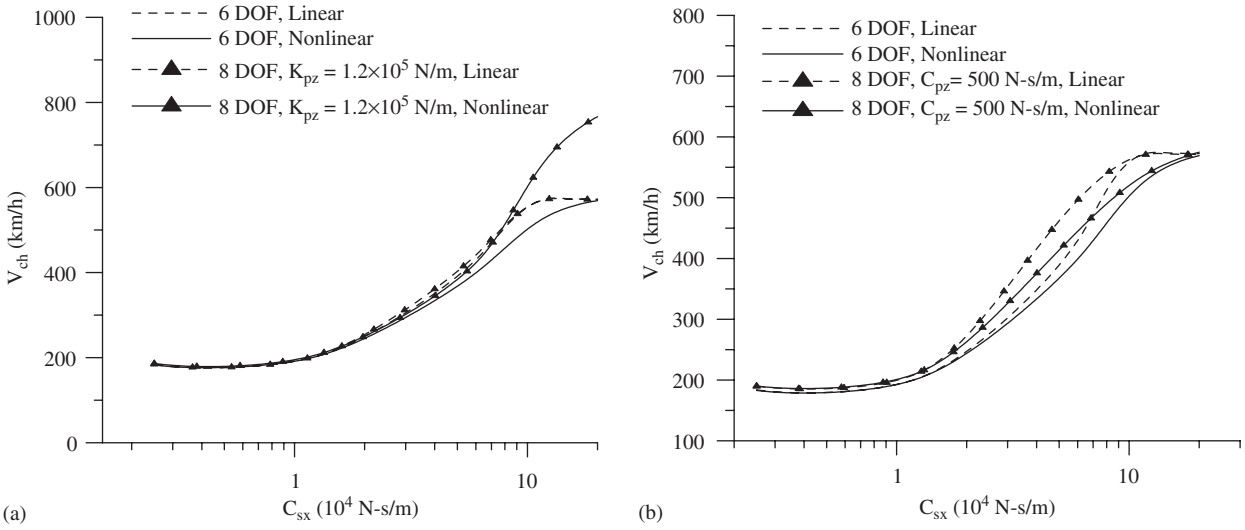

Fig. 4. The influence of the longitudinal damping of the secondary suspension C_{sx} on the critical speeds of a truck evaluated via the various degrees of freedom with the linear and the nonlinear creep models when (a) $C_{pz} = 1.44 \times 10^4$ N s/m, and (b) $K_{pz} = 2.0 \times 10^5$ N/m.

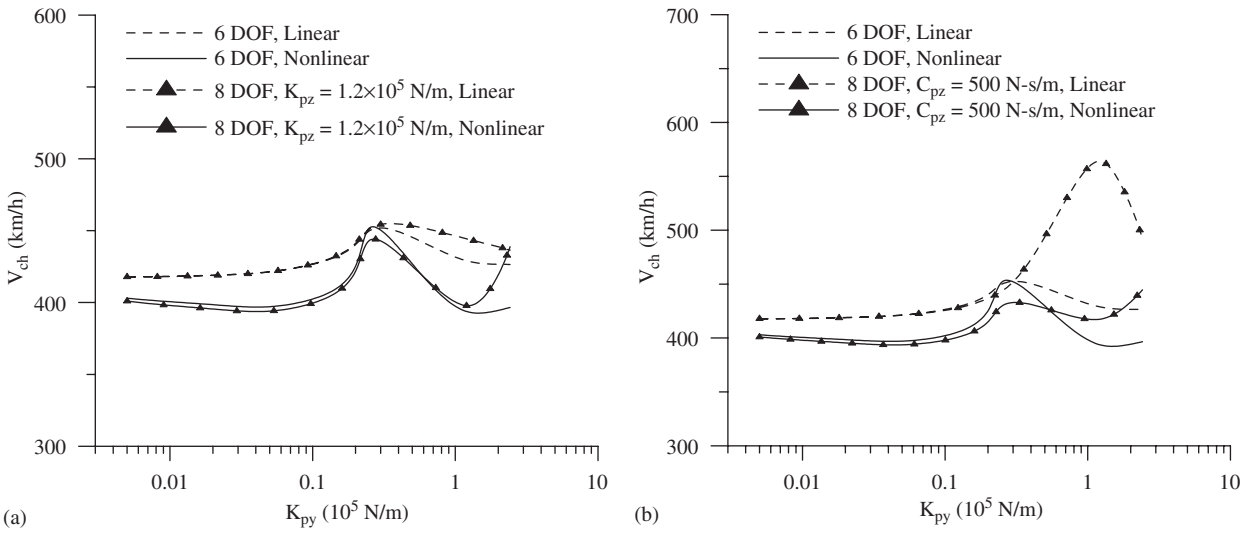

Fig. 5. The influence of the lateral stiffness of the primary suspension K_{py} on the critical speeds of a truck evaluated via the various degrees of freedom with the linear and the nonlinear creep models when (a) $C_{pz} = 1.44 \times 10^4$ N s/m, and (b) $K_{pz} = 2.0 \times 10^5$ N/m.

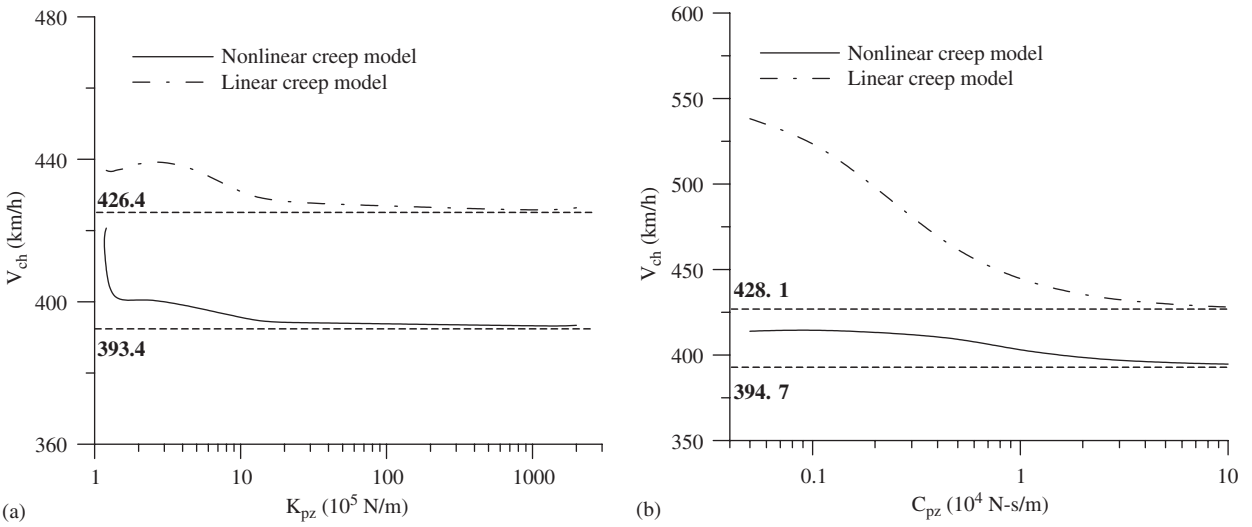

Fig. 6. The influence of (a) the vertical stiffness K_{pz} and (b) the vertical damping C_{pz} of the primary suspension on the critical speed evaluated via the linear and the nonlinear creep models.

evaluated by the nonlinear creep model. However, based on the system data given in Fig. 4a, it is observed that when C_{sx} is greater than 8×10^4 N s/m, the critical hunting speeds of an 8dof system evaluated by the linear creep model are lower than those evaluated by the nonlinear creep model.

Fig. 5 reveals that the influence on the critical hunting speeds of the lateral stiffness of the primary suspension, K_{py}, depends upon the particular modeling system considered. It shows that the critical speeds increase first then decrease as K_{py} increases. In most of the cases, the critical hunting speeds evaluated by the linear creep model are higher than those evaluated by the nonlinear creep model. For the two creep models, the critical hunting speeds evaluated via the 6dof system are higher than those evaluated via the 8dof system when K_{py} is small. However, this relationship is inverted as K_{py} is further large.

In Fig. 6, the influence of the vertical stiffness, K_{pz}, and the vertical damping, C_{pz}, of the primary suspension on the critical hunting speeds evaluated by the linear and the nonlinear creep models are illustrated. It is observed that the critical hunting speed decreases as K_{pz} and C_{pz} increase for these two models. Meanwhile, it can be found that the critical hunting speed evaluated via the linear creep model is higher than those evaluated via the nonlinear creep model. Moreover, when K_{pz} and C_{pz} approaches infinity, the critical hunting speeds will converge to the fixed values evaluated via the 6dof system. When K_{pz} and C_{pz} are small, the difference between the critical hunting speeds evaluated via the 6dof and the 8dof systems are large. This can also be clearly found and validated in Figs. 3–5.

5. Conclusion

In this paper, based on the heuristic nonlinear creep model, the coupled nonlinear governing differential equations of motion of an 8dof truck system moving on curved tracks, are derived in completeness. In the limiting study, the reduced governing differential equations of motion of a truck are shown to be consistent with those in the existing literature. It is found that in most of cases, the critical hunting speeds evaluated via the 8dof system moving on curved tracks are higher than those evaluated via the 6dof system. The critical hunting speeds evaluated via the linear creep model are greater than that evaluated via the nonlinear creep model. The influences of the physical parameters, the vertical stiffness and the vertical damping of the primary suspension, not considered in the 6dof system on the critical hunting speeds are investigated. According to the influence of K_{pz} and C_{pz} on the critical hunting speeds, it can be seen that the 8dof system can be reduced to the 6dof system as the rigidity of the primary suspension in the vertical direction increases.

Acknowledgment

This research work was sponsored by the National Science Council of Taiwan, R.O.C. under Grant NSC92-2212-E-006-073.

Appendix. Data of the system parameters [18,19]

Parameters	Value
Wheelset mass (kg)	$m_w = 1117.9$
Bogie frame mass (kg)	$m_t = 350.26$
Roll moment of the inertia of the wheelset (kg m^2)	$I_{wx} = 608.1$
Spin moment of the inertia of the wheelset (kg m^2)	$I_{wy} = 72$
Yaw moment of the inertia of the wheelset (kg m^2)	$I_{wz} = 608.1$
Roll moment of the inertia of the bogie frame (kg m^2)	$I_{tx} = 35$
Yaw moment of the inertia of the bogie frame (kg m^2)	$I_{tz} = 105.2$
Wheel radius (m)	$r_0 = 0.43$
Half of the track gauge (m)	$a = 0.7175$
Wheel conicity	$\lambda = 0.05$
Half of the primary longitudinal spring arm (m)	$b_1 = 1.0$
Half of the primary longitudinal damping arm (m)	$b_1 = 1.0$
Half of the primary vertical spring arm (m)	$b_1 = 1.0$
Half of the primary vertical damping arm (m)	$b_1 = 1.0$
Half of the secondary longitudinal spring arm (m)	$b_2 = 1.18$
Half of the secondary longitudinal damping arm (m)	$b_3 = 1.4$
Half of the primary lateral spring arm (m)	$L_1 = 1.28$
Half of the primary lateral damping arm (m)	$L_2 = 1.5$
Vertical distance from the wheelset center of the gravity to the secondary suspension (m)	$h_T = 0.47$
Longitudinal stiffness of the primary suspension (N/m)	$K_{px} = 9 \times 10^5$
Lateral stiffness of the primary suspension (N/m)	$K_{py} = 2.4 \times 10^5$
Vertical stiffness of the primary suspension (N/m)	$K_{pz} = 2.4 \times 10^5$
Vertical damping of the primary suspension (N s/m)	$C_{pz} = 1.44 \times 10^4$
Longitudinal stiffness of the secondary suspension (N/m)	$K_{sx} = 4.5 \times 10^3$
Lateral stiffness of the secondary suspension (N/m)	$K_{sy} = 4.5 \times 10^3$
Longitudinal damping of the secondary suspension (N s/m)	$C_{sx} = 6 \times 10^4$
Lateral damping of the secondary suspension (N s/m)	$C_{sy} = 1.8 \times 10^3$
Lateral rail stiffness (N/m)	$K_r = 1.617 \times 10^7$
Flange clearance (m)	$\delta = 0.00923$
Lateral creep force coefficient (N)	$f_{11} = 2.212 \times 10^6$
Lateral/spin creep force coefficient (N m^2)	$f_{12} = 3120$
Spin creep force coefficient (N)	$f_{22} = 16$
Longitudinal creep force coefficient (N)	$f_{33} = 2.563 \times 10^6$
Radius of curved tracks (m)	$R = 6250$
Superelevation angle of curved track (rad)	$\phi_{se} = 0.0873$
Axle load (N)	$W = 5.6 \times 10^4$
Coefficient of the friction	$\mu = 0.2$
Normal force of the wheelset at the equilibrium state (N)	$N = W/2$

References

[1] A.H. Wickens, The dynamic stability of railway vehicle wheelsets and bogies having profiled wheels, *International Journal of Solids and Structures* 1 (1965) 319–341.

[2] D. Horak, D.N. Wormley, Nonlinear stability and tracking of rail passenger trucks, *ASME Journal of Dynamic Systems, Measurement, and Control* 104 (1982) 256–263.

[3] A.H. Wickens, Static and dynamic instabilities of bogie railway vehicles with linkage steered wheelsets, *Vehicle System Dynamics* 26 (1996) 1–16.

[4] A. Mehdi, Y. Shaopu, Effect of system nonlinearities on locomotive bogie hunting stability, *Vehicle System Dynamics* 29 (1998) 366–384.

[5] S.Y. Lee, Y.C. Cheng, Hunting stability analysis of high-speed railway vehicle trucks on tangent tracks, *Journal of Sound and Vibration* 282 (3–5) (2005) 881–898.

[6] H. Scheffel, R.D. Fröhling, P.S. Heyns, Curving and stability analysis of self-steering bogies having a variable yaw constraint, in: *Vehicle System Dynamics Proceedings of the 13th IAVSD Symposium on the Dynamics of Vehicles on Roads and on Tracks*, vol. 23(Suppl.), 1993, pp. 425–436.

[7] A.H. Wickens, Static and dynamic stability of unsymmetric two-axle railway vehicles possessing perfect steering, *Vehicle System Dynamics* 11 (1982) 89–106.

[8] A.H. Wickens, Railway vehicles with generic bogies capable of perfect steering, *Vehicle System Dynamics* 25 (1996) 389–412.

[9] C.E. Bell, D. Horak, Forced steering of rail vehicles: stability and curving mechanics, *Vehicle Systems Dynamics* 10 (1981) 357–386.

[10] Y. Suda, High speed stability and curving performance of longitudinally unsymmetric trucks with semi-active control, *Vehicle Systems Dynamics* 23 (1994) 29–51.

[11] Y. Suda, T. Fujioka, M. Iguchi, Dynamic stability and curving performance of railway vehicles, *Bulletin of the JSME* 29 (256) (1986) 3538–3544.

[12] T. Fujioka, Y. Suda, M. Iguchi, Representation of railway suspensions of rail vehicles and performance of radical trucks, *Bulletin of the JSME* 27 (1984) 2249–2257.

[13] S.S. Narayana, R.V. Dukkipati, M.O.M. Osman, A comparative study on lateral stability and steady state curving behaviour of unconventional rail truck models, Proceedings of the Institution of Mechanical Engineers Part F. *Journal of Rail and Rapid Transit* 208 (1994) 1–13.

[14] R.V. Dukkipati, S.S. Narayana, Lateral stability and steady state curving performance of unconventional rail trucks, *Mechanism and Machine Theory* 36 (2001) 577–587.

[15] R.V. Dukkipati, S.S. Narayana, M.O.M. Osman, Curving analysis of modified designs of passenger railway vehicle trucks, *JSME International Journal Series C: Mechanical Systems, Machine Elements and Manufacturing* 25 (1) (2002) 159–167.

[16] S.Y. Lee, Y.C. Cheng, Nonlinear hunting stability analysis of high speed railway vehicles on curved tracks, heavy vehicle system, *International Journal of Vehicle Design* 10 (4) (2003) 344–361.

[17] R.V. Dukkipati, V.K. Garg, *Dynamics of Railway Vehicle Systems*, Academic Press, Canada, 1984.

[18] M. Vidyasager, *Nonlinear Systems Analysis*, Prentice-Hall, Englewood Cliffs, NJ, 1978.

[19] A.K.W. Ahmed, S. Sankar, Lateral stability behavior of railway freight car system with elasto-damper coupled wheelset: Part 2—truck model, *Transactions of the ASME, Journal of Mechanisms, Transmissions and Automation in Design* 109 (4) (1987) 500–507.

[20] T. Hirotsu, K. Terada, M. Hiraishi, S. Yui, Simulation of hunting of rail vehicles (the case using a compound circular wheel profile), *JSME International Journal Series III, Vibration, Control Engineering, Engineering for Industry* 34 (3) (1991) 396–403.